sciendo

POLISH MARITIME RESEARCH 2 (122) 2024 Vol. 31; pp. 4-12
10.2478/pomr-2024-0016

Investigation of the Scale Effects on Roll Motion for The Ship *Bettica* Using Numerical Simulation

Nguyen Thi Ha Phuong *
Naofumi Yoshida
Tomoki Taniguchi
Toru Katayama
Osaka Metropolitan University, Graduate School of Engineering, Department of Marine System Engineering, Japan

* Corresponding author: *su22435l@st.omu.ac.jp (Nguyen Thi Ha Phuong)*

ABSTRACT

In this paper, we focus on analysing scale effects on the roll motion of the Italian ship Bettica using a numerical method. First, the roll decay motion of the ship is simulated at both the model scale and full scale, and the predicted results are compared with experimental data to validate the numerical strategy. The results show that there are scale effects that cause the difference in roll amplitudes between the model and the full-scale ship. To investigate the viscous effects on the roll damping components, forced roll simulations are carried out at the model scale and full scale, and the roll damping components (frictional, wave-making, eddy-making, bilge keel and lift components) are obtained. An analysis of these roll damping components indicates that the frictional component is influenced by scale effects, especially in the case of zero or low forward speed. We also show that the bilge keel component is affected by scale effects when the height of the bilge keels is reduced to a certain value below the boundary layer thickness. The velocity fields around the bilge keels are analysed to better understand the scale effects.

Keywords: scale effects, roll decay, forced roll, roll damping coefficients, full-scale roll motion

INTRODUCTION

Until now, the impact of scale effects on roll motion has been undetermined, due to the difficulty of conducting full-scale tests. However, with the aid of computational tools such as computational fluid dynamics (CFD), full-scale roll damping can be calculated by numerical methods, although the results need to be validated and sea trial data are scarce.

For these reasons, there is a limited number of research works that deal with this problem. According to Himeno, scale effects on roll damping are mainly related to skin friction damping, which accounts for a small proportion of the total roll damping [1]. Grant [2] carried out full-scale roll decay tests in sea trials in calm water, and recorded the flow field using a Particle Image Velocimetry (PIV) method for the Italian ship *Bettica*. Using the same research object, experiments and numerical simulations of roll decay motion were carried out by Broglia et al. [3] at different Froude and Reynolds numbers. Although the full-scale and model-scale results from numerical and experimental methods were compared, the scale effects were not clearly demonstrated in this paper, and the numerical simulations underpredicted the roll motion for low forward speeds due to insufficient grid resolution. In a study by Kianejad et al. [4], the full-scale and model-scale roll characteristics and damping coefficients were simulated under different conditions for a container ship using a harmonic excited roll motion (HERM) technique to analyse the scale effects. One drawback of this study was that the full-scale numerical results were not validated

against sea trial data. In a study by Carl-Johan Söder et al. [5], it was shown through model-scale and full-scale experiments that the full-scale damping was slightly higher than in the model tests, and that this should be further investigated. The studies described above confirm that the accurate simulation of roll motion using CFD is necessary in order to investigate scale effects, as this method is not limited by the size of the object, although the results need to be validated to ensure reliability. In addition, as the scale effects on roll motion may not be clear, it is important to study these with more accurate calculations to develop a better understanding.

In this paper, we aim to clarify the scale effects on the roll motion of the Italian ship *Bettica* using a numerical method. First, the roll decay motion is simulated at both the model scale and the full scale, and the numerical strategy is validated by comparing the CFD results with experimental and sea trial data. Roll decay tests are then simulated under other conditions at the model scale and full scale to investigate the impact of scale effects on roll motion. Following this, in order to investigate viscous effects on the roll damping components, forced roll simulations are carried out at the model scale and full scale, and the roll damping components are obtained. Finally, the bilge keel component is analysed in the case where the height of the bilge keel is reduced, and the velocity fields around the bilge keels are observed to gain a full understanding of the physical phenomena associated with scale effects.

NUMERICAL SIMULATION

THE *BETTICA*

The simulation object in this study is the ship *Bettica* (P-492). This is the third vessel in the Commandante class of light combatant vessels, and was built for the Italian Navy at the Riva Trigoso shipyard [6]. The ship has two propeller axes, two rudders, bilge keels, and active fins. Sea trials of the ship including roll decay tests in calm water were conducted in October 2007 in the Mediterranean Sea [2]. Roll decay tests in calm water were also carried out for a fully appended model (scale factor 20) at the Italian Ship Model Basin (INSEAN), and the experimental results can be found in the paper by Broglia [3]. A photo of the *Bettica* with the 3D model and the main parameters of the ship are shown in Fig. 1 and Table 1, respectively.

Tab. 1. Main parameters of the Bettica (full appendages)

Parameter	Symbol	Units	Ship	Model
Scale factor	λ	-	1	20
Maximum length	L_{max}	m	88.6	4.43
Length between perpendiculars	L_{pp}	m	80	4.0
Breadth	B	m	12.2	0.61
Draft	d	m	3.2	0.16
Block coefficient	C_B	-	0.455	0.455
Mass	W	t	1399	0.174
Metacentric height	GM	m	1.107	0.055
Moment of inertial in X direction	I_{xx}	kg.m^2	2.5x10^7	7.52
Moment of inertial in Y, Z directions	I_{yy}, I_{zz}	kg.m^2	5.6x10^8	174.8
Natural roll period	T_r	s	9.65	2.3

NUMERICAL SETUP

Full-scale and model-scale roll motion simulations in calm water were carried out using CFD commercial software STAR-CCM+ (version 18.02.010-R8) based on the unsteady Reynolds averaged Navier–Stokes (URANS) equations. The simulation conditions, such as the forward speed, roll amplitude, and number of degrees of freedom (DOF), varied in each case, and will be described later.

In this study, the overset mesh method was used to simulate the roll motion at both the model scale and the full scale in view of its advantages over other mesh techniques, which have been shown in many studies [7] [8]. The computational domain consists of two regions, the background and overset, which are connected by an overset mesh interface. To simulate the roll motion, the overset region is set to rotate around the roll axis. Here, the roll axis is defined as the longitudinal axis passing through the ship's centre of gravity. The virtual towing tank (background region) is set to a large enough value to avoid wave reflections, which could affect the results. The size of the background and overset regions and the boundary conditions are shown in Fig. 2.

In the CFD simulations, the volume of fluid (VOF) method was used for multiphase flow to solve for the interfaces between the water and air at the free surface, and the implicit unsteady solver was selected to solve for the flow field around the ship. The all-y+ wall treatment method was used to simulate the high-wall treatment for coarse meshes and the low-wall treatment for fine meshes. The SST k-ω model was selected as the turbulence

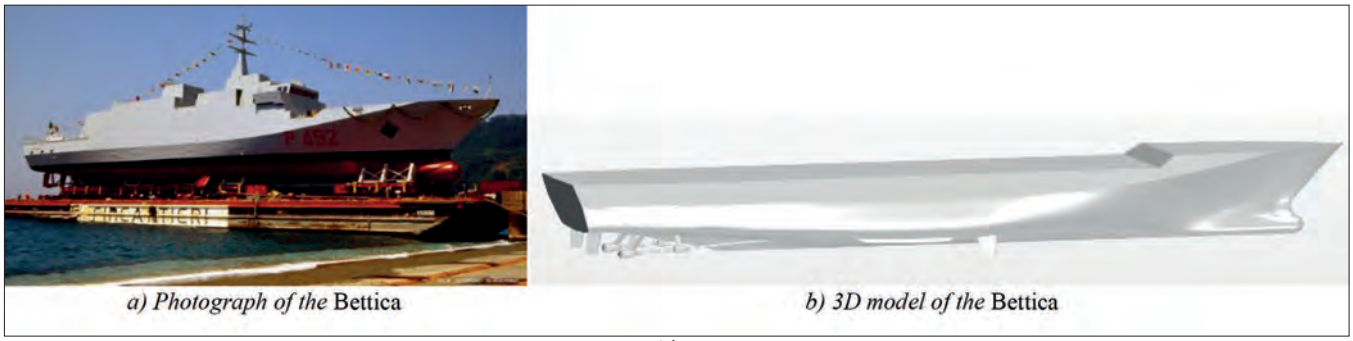

a) Photograph of the Bettica *b) 3D model of the* Bettica

Fig. 1. The Bettica

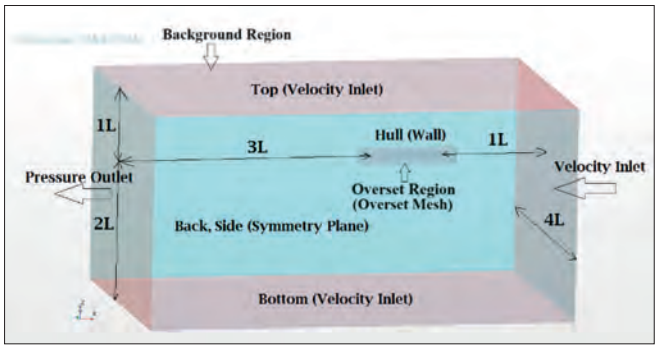

Fig. 2. Computational domain and boundary conditions

model, as it offers better predictions of flow separation under adverse pressure gradients and gives more accurate results [9].

At the mesh generation stage, surface remesher, trimmer and prism layers along the wall were used for the background and overset regions, as these three meshing models with their own functions helped to model the near-wall flow and to resolve the boundary layer accurately. When setting the grid parameters, finer meshes were required in certain areas using different mesh blocks to reduce the number of grid cells, thereby reducing the running time. In this case, the meshes were refined in the regions near the bow, stern, appendage and around the hull in order to capture the roll motion more accurately (Fig. 3). Grids were created from coarse to fine by reducing the base size of the mesh.

In this study, the average wall y+ value was set to below 2.5 for the model-scale simulations, according to the ITTC recommendations [10], and to 100–200 for the full-scale simulations (this range of values has been proven to be suiTable for full-scale simulations in many studies [11] [12] [13] [14]). The time step for the URANS simulations depends on the properties of the flow [15]. The ITTC recommends [16] that at least 100 time steps should be used per roll period for roll motion simulations. However, in the present paper, the time step scheme was based on the Courant number, giving values that were much smaller than the ITTC recommendations, with time steps of 0.014 s (=T_r/160) and 0.04 s (=T_r/250) for the model-scale and full-scale simulations, respectively.

ROLL DECAY SIMULATIONS

In this section, we describe model-scale and full-scale simulations of the roll decay motions of the fully appended ship (where the active fins and rudders are not operational). A mesh and time step sensitivity study is presented, and the numerical results and experimental data are compared in order to validate the accuracy of the numerical method. The roll decay motions of the model-scale and full-scale ships are compared to explore the scale effects.

MESH AND TIME STEP CONVERGENCE STUDY

A convergence study of the mesh size and time step was conducted according to the ITTC Recommended Procedures and Guidelines (2008) [17]. The GCI method [18] was used to calculate the convergence ratio (R_i) and the grid convergence index (*GCI*). A refinement ratio of $r_i = \sqrt{2}$ was used to create three solutions.

Mesh and time step sensitivity studies were carried out with three solutions, referred to here as fine ($S_{i,1}$), medium ($S_{i,2}$), and coarse ($S_{i,3}$). The changes in the solution between medium to fine ($\varepsilon_{i,21}$) and coarse to medium ($\varepsilon_{i,32}$) and the convergence ratio (R_i) are defined as follows:

$$\varepsilon_{i,21} = S_{i,2} - S_{i,1} \tag{1}$$

$$\varepsilon_{i,32} = S_{i,3} - S_{i,2} \tag{2}$$

$$R_i = \varepsilon_{i,21}/\varepsilon_{i,32} \tag{3}$$

Three convergence conditions are possible: monotonic convergence ($0< R_i <1$), oscillatory convergence ($R_i <0$), and divergence ($R_i >1$). For monotonic convergence, the order of accuracy (p_i), the error (δ_{RE}), and the grid convergence index (*GCI*) are defined as follows:

$$p_i = \frac{ln(\varepsilon_{i,32} - \varepsilon_{i,21})}{ln(r_i)} \tag{4}$$

$$\delta_{RE} = \frac{\varepsilon_{i,21}}{r_i^{p_i} - 1} \tag{5}$$

$$GCI^{21} = \frac{F_s \cdot \varepsilon_{i,21}}{S_{i,1} \cdot (r_i^{p_i} - 1)} = \frac{F_s \cdot |\delta_{RE}|}{S_{i,1}} \tag{6}$$

where F_s is the factor of safety ($F_s = 1.25$ for all three solutions).

The simulation conditions for the model-scale and full-scale ships are summarised in Table 2. These conditions were decided based on the experimental results [3] and sea trial data [2], which were used to validate the numerical simulation. For the free roll decay simulations, we considered three peak values ($t_1 \approx 5.3$ s, $t_2 \approx 6.85$ s, and $t_3 \approx 8.5$ s for the model-scale ship and $t_1 \approx 14.5$ s, $t_2 \approx 19.2$ s, and $t_3 \approx 23.8$ s for the full-scale ship) at the front, middle, and aft of the roll decay curves, respectively, to calculate the convergence ratio. Different solutions for the mesh size and

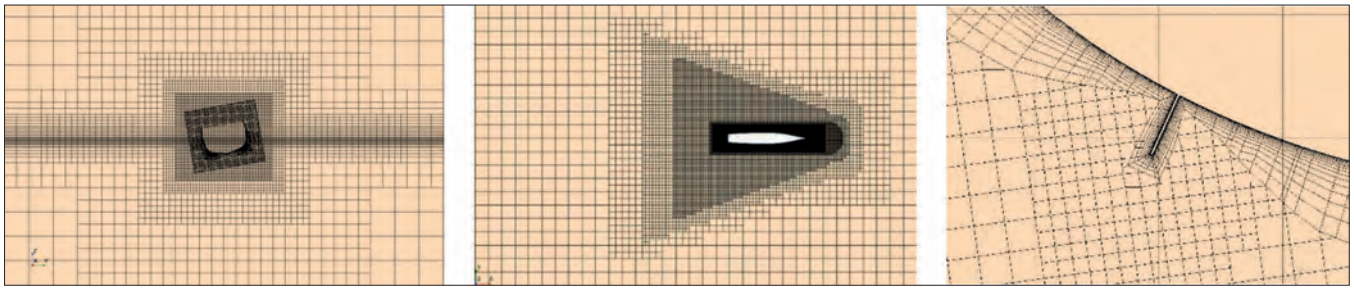

Fig. 3. Meshes generated in different areas of the ship

time step as well as the number of grid cells for the model-scale and full-scale ships are shown in Table 3. Table 4 shows the results of the grid and time step convergence study. Validation of the roll decay simulation results under different conditions is shown in Fig. 4, in which the model-scale CFD results are compared with the Experimental Fluid Dynamics (EFD) result [3], and the full-scale CFD results are compared with full-scale data [2].

Tab. 2. Simulation conditions for the roll decay tests

Conditions	Model scale	Full scale
Draft [m]	0.1685	3.2
Froude number (Fr)	0.166; 0.227	0.193; 0.276
Initial roll angle [degree]	10	8; 9
Number of degrees of freedom	3 DOF (heave, pitch, roll)	6 DOF

Tab. 3. Cases for the mesh and time step convergence study

Model scale			Full scale		
Base size [m]	Time step [m]	Grid cells [mil. cells]	Base size [m]	Time step [m]	Grid cells [mil. cells]
0.17	0.014	1.08	2.55	0.04	2.07
0.12	0.014	2.14	1.8	0.04	4.2
0.085	0.014	4.25	1.27	0.04	7.6
0.12	0.02	2.14	1.8	0.08	4.2
0.12	0.01	2.14	1.8	0.06	4.2

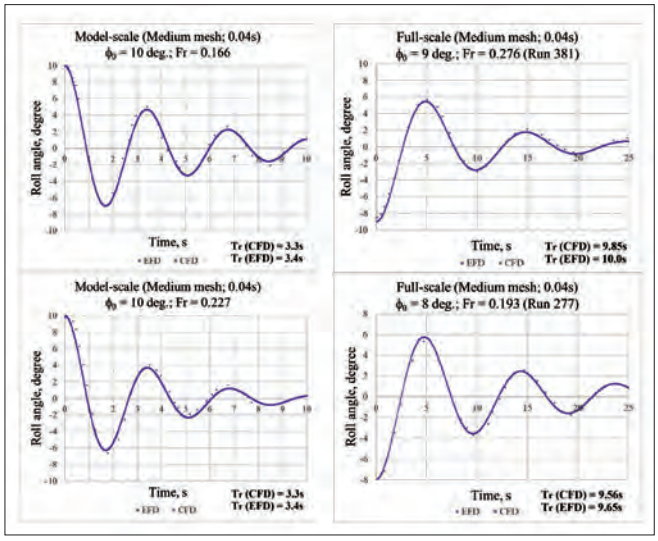

Fig. 4. Results for the CFD and EFD roll decay motions

As can be seen from Table 4, monotonic convergence was achieved for all combinations of mesh size and time step. The result for the grid convergence index $GCI^{21} < GCI^{32}$ indicates that the discretisation error due to the grid and time step is reduced, and an independent solution is achieved. The medium-sized grid and a medium time step can therefore be used to simulate the roll decay motion to save computational time. The results in Fig. 4 indicate that the model-scale and

Tab. 4. Results of the mesh and time step convergence study

Model scale (10 deg.; Fr = 0.277)									
t_1 = 5.3 s									
Symbol	$S_{i,3}$	$S_{i,2}$	$S_{i,1}$	$\varepsilon_{i,21}$	$\varepsilon_{i,32}$	R_i	p_i	GCI^{21}	GCI^{32}
Mesh size	2.134	2.023	2.022	0.001	0.111	0.009	13.589	0.001	0.062
Time step	2.055	2.199	2.244	−0.045	−0.144	0.312	3.362	1.136	3.717
t_2 = 6.85 s									
Symbol	$S_{i,3}$	$S_{i,2}$	$S_{i,1}$	$\varepsilon_{i,21}$	$\varepsilon_{i,32}$	R_i	p_i	GCI^{21}	GCI^{32}
Mesh size	1.387	1.255	1.196	0.059	0.132	0.449	2.309	5.057	10.724
Time step	1.212	1.321	1.349	−0.029	−0.109	0.263	3.858	0.944	3.671
t_3 = 8.5 s									
Symbol	$S_{i,3}$	$S_{i,2}$	$S_{i,1}$	$\varepsilon_{i,21}$	$\varepsilon_{i,32}$	R_i	p_i	GCI^{21}	GCI^{32}
Mesh size	0.868	0.766	0.704	0.062	0.102	0.611	1.423	17.366	26.120
Time step	0.714	0.792	0.809	−0.017	−0.078	0.217	4.407	0.728	3.427
Full scale (8 deg; Fr = 0.193)									
t_1 = 14.5 s									
Symbol	$S_{i,3}$	$S_{i,2}$	$S_{i,1}$	$\varepsilon_{i,21}$	$\varepsilon_{i,32}$	R_i	p_i	GCI^{21}	GCI^{32}
Mesh size	2.625	2.486	2.484	0.002	0.139	0.014	12.238	0.001	0.102
Time step	2.367	2.423	2.476	−0.053	−0.056	0.946	0.159	47.270	51.039
t_2 = 19.2 s									
Symbol	$S_{i,3}$	$S_{i,2}$	$S_{i,1}$	$\varepsilon_{i,21}$	$\varepsilon_{i,32}$	R_i	p_i	GCI^{21}	GCI^{32}
Mesh size	1.649	1.618	1.589	0.029	0.031	0.935	0.192	33.08	34.727
Time step	1.632	1.665	1.670	−0.005	−0.033	0.152	5.445	0.067	0.442
t_3 = 23.8 s									
Symbol	$S_{i,3}$	$S_{i,2}$	$S_{i,1}$	$\varepsilon_{i,21}$	$\varepsilon_{i,32}$	R_i	p_i	GCI^{21}	GCI^{32}
Mesh size	1.237	1.119	1.091	0.028	0.118	0.237	4.151	0.998	4.101
Time step	1.254	1.270	1.285	−0.015	−0.016	0.937	0.186	21.887	23.622

full-scale roll decay motions under different conditions obtained from the numerical simulations show good alignment with measurements. Moreover, the differences between CFD and EFD average natural roll periods (T_r) at the full scale and model scale are insignificant. This means that the simulation strategy in this study is reliable and can be used for other conditions, as described in the next sections.

SCALE EFFECTS ON ROLL DECAY MOTION

In this section, we simulate and compare the model-scale and full-scale roll decay motion of a ship with bilge keels to explore the effects of scale on roll motion. The same simulation conditions are considered for both the model-scale and full-scale ships (Table 4). To investigate the scale effects accurately, the correspondence in the numerical simulations between the model-scale and full-scale ships should be determined based on the correspondence in mesh size, time step, Courant number and wall y+ value. In this study, a medium-sized mesh and time step (with Courant number < 1) are used for both the model-scale and full-scale simulations, and wall y+ values of 2.5 and 150 are set for the model-scale and full-scale ships, respectively. To compare the roll motion between the full-scale ship and the model, the time is expressed in the same units of t/T_r. The extinction coefficient can be calculated from the roll decay curves (the details of the calculation method are given in [19]). Fig. 5 shows a comparison of the roll decay CFD results and the extinction coefficient between the ship and model. It can be seen that there are scale effects that cause the difference in roll amplitudes and extinction coefficients between the model-scale and full-scale ships. The effects are largest in the case of zero forward speed, and are insignificant at high speeds. These effects are discussed in the next section.

Tab. 5. Simulation conditions (ship with bilge keels)

Conditions	Model scale	Full scale
Draft [m]	0.16	3.2
Froude number (Fr)	0; 0.193	0; 0.193
Initial roll angle [degree]	8	8
Number of degrees of freedom	1 DOF (roll)	1 DOF (roll)

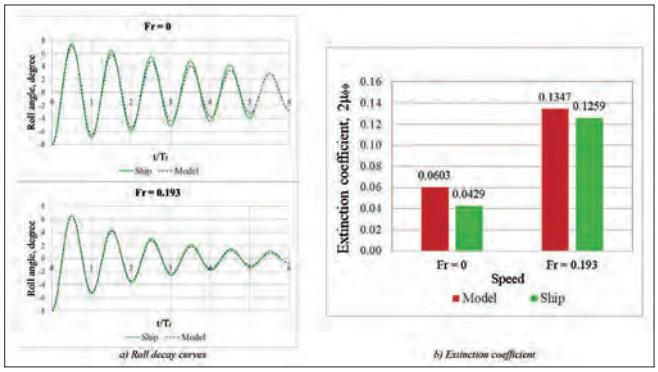

Fig. 5. Roll decay CFD results and extinction coefficient (comparison between ship and model)

FORCED ROLL SIMULATIONS

In this section, we present the results for forced roll motions of the ship and model with bilge keels, and analyse the scale effects on the roll damping components. The roll damping coefficients are calculated and the velocity fields around the bilge keels are observed. The simulation conditions are the same as in Table 4.

CALCULATION OF ROLL DAMPING COEFFICIENTS

The roll damping coefficient can be calculated from the forced roll simulation (the details of this process are given in [20]). For the CFD simulation, the overset region was subjected to forced rolling by a harmonic oscillation as follows:

$$\phi(t) = \phi_a \sin(\omega t) \tag{7}$$

where ϕ_a is the roll amplitude, and ω is the roll frequency. A start-up function $f(t)$ was applied to avoid strong transient flows at the earlier time steps in the calculation, which can affect the accuracy of the results. The time history of the roll amplitude is defined by:

$$\phi(t) = f(t)\phi_0 \sin(\omega t) \tag{8}$$

$$f(t) = \begin{cases} \frac{1}{2}\sin\left(\frac{1}{4}\times\frac{\pi}{T_r}\times t - \frac{1}{2}\pi\right) + \frac{1}{2} & (t<4T_r) \\ 1 & (t>4T_r) \end{cases} \tag{9}$$

Based on the time history of exciting moments (M_E), the equation for the roll moment can be expressed (using a Fourier series expansion) as follows:

$$M_E = M_0.\sin(\omega t + \varepsilon) \tag{10}$$

where M_0 is the equivalent linear amplitude of the roll moment, and ε is the phase difference between the roll angle and roll moment. The equivalent linear roll damping coefficient (b_{44}) and its non-dimensional coefficient (B_{44}) are then defined as follows:

$$b_{44} = \frac{M_0.\sin(\varepsilon)}{\phi_0 \omega}; \quad B_{44} = \frac{b_{44}}{\nabla \rho B^2}\sqrt{\frac{B}{2g}} \tag{11}$$

where ∇ is the displacement volume of the ship, g is the gravitational acceleration, and ρ is the density of water.

According to a study by Ikeda [21], roll damping can be assumed to consist of five components: the frictional, wave making, eddy making, lift and bilge keel components. From the forced roll simulation, the time history of the frictional moment and bilge keel moment can be obtained. In general, the bilge keel damping component can be calculated by subtracting the roll moment from the simulations with and without bilge keels. For a ship with a slender shape, such as the *Bettica*, the hull pressure component of the bilge keel damping component is not large. Hence, in this study, B_{44BK}

can be calculated by Eq. (12), based on the time history of the bilge keel moment. Using a Fourier series expansion, the amplitudes of the frictional moment (M_{0F}) and bilge keel moment (M_{0BK}) and their phase differences (ε_F, ε_{BK}) can be obtained, and the frictional damping coefficient (b_{44F}) and bilge keel damping coefficient (b_{44BK}) are calculated in a similar way as in Eqs. (10) and (11). The frictional damping coefficient (B_{44F}) and bilge keel damping coefficient (B_{44BK}) are calculated in non-dimensional form as follows:

$$B_{44F} = \frac{b_{44F}}{\nabla \rho B^2}\sqrt{\frac{B}{2g}}; \quad b_{44F} = \frac{M_{0F}.\sin(\varepsilon_F)}{\phi_0 \omega};$$
$$B_{44BK} = \frac{b_{44BK}}{\nabla \rho B^2}\sqrt{\frac{B}{2g}}; \quad b_{44BK} = \frac{M_{0BK}.\sin(\varepsilon_{BK})}{\phi_0 \omega} \tag{12}$$

The other roll damping components (wave making, eddy making, and lift) are considered as a single coefficient, which is defined as:

$$B_{44W} + B_{44E} + B_{44L} = B_{44} - B_{44F} - B_{44BK} \tag{13}$$

SCALE EFFECTS ON ROLL DAMPING COMPONENTS

As stated above, model-scale and full-scale forced roll simulations were carried out for the *Bettica* at zero speed with bilge keels and a forward speed of 10 kts (Fr = 0.193). The results for the roll damping components and their contributions (%) are shown in Fig. 6. It can be seen that the frictional damping coefficient at the model scale is larger than that at full scale, and that this component is larger in the case of zero forward speed. The other components are not affected by the scale effects. The percentage of the bilge keel damping component decreases with an increase in forward speed (due to the increase in the lift damping component). The percentage of the frictional damping component at the model scale is higher than at the full scale. In the case of zero speed, the frictional damping component accounts for a larger proportion (14.04%) at the model scale and is only 6.17% at the full scale. By comparing the full-scale and model-scale results, we see that the total roll damping coefficient of full-scale ship is smaller than that of model-scale in all cases, as the frictional damping coefficient is lower (the viscous effects are lower) at higher Reynolds numbers.

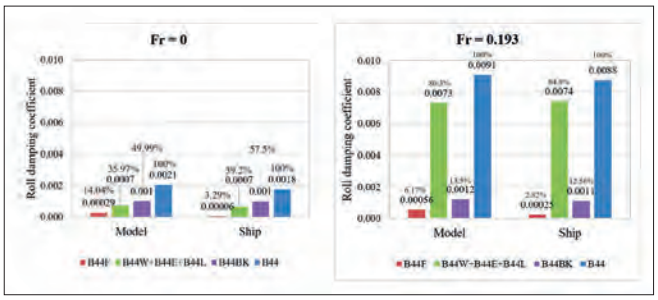

Fig. 6. Roll damping coefficients and their contributions (comparison between ship and model)

SCALE EFFECTS FOR REDUCED BILGE KEEL HEIGHT

According to a previous study by Katayama et al. [22], an insufficient height of the bilge keel compared to the boundary layer thickness may cause scale effects on bilge keel damping. To investigate the scale effects on the bilge keel component, the height of the bilge keel ($h = h_{BK}$) was reduced to 70% and 50% of the design value. In the CFD simulations, the prism layer thickness, number of prism layers and prism layer stretching were selected to obtain the desired wall y+, which is defined as $y^+ = (y/v)\sqrt{\tau_w/\rho}$, where v is the kinematic viscosity of water, τ_w is the mean wall shear stress, and y is the distance of the cell centroid from the wall. The boundary layer thickness (δ_{99}) can be estimated as $\delta_{99} = 0.37L/(Re^{1/5})$ using the Blasius solution for turbulent flow [23]. Theoretically, the total prism layer thickness should be equal to δ_{99} so that the gradients in the boundary layer can be captured. However, we note that since this estimation is based on the theory of turbulent flow over a flat plate, without an applied pressure gradient, real CFD simulations using a different geometry should be adjusted according to the mesh quality criteria. Hence, the boundary layer was generated by setting the prism layer stretching to around 1.2, with 20 prism layers for both the model-scale and full-scale ships, and with a prism layer thickness equal to 0.02 m and 0.3 m at the model scale and the full scale, respectively. The values for the bilge keel height and boundary layer thickness are given in Table 6. The results for the roll damping coefficients are shown in Fig. 7. The relation between the bilge keel damping coefficient and the ratio of the bilge keel height to the boundary layer thickness is given in Fig. 8. To better understand the scale effects, the velocity fields around the naked hull and velocity fields around the bilge keels of the ship and model, for both the full bilge keel height and half height, were observed over a half roll cycle (Figs. 9–11). A comparison of the velocity distributions in the boundary layers between the ship and the model (Fr = 0.193) is given in Fig. 12.

The results indicate that when the bilge keel height is reduced to a certain value that is smaller than the boundary layer thickness ($h/\delta < 1$), the bilge keel damping component is affected by scale effects. The bilge keel damping coefficient decreases with the bilge keel height, and is larger for the full-scale ship than at the model scale. In addition, the scale effects are larger in the case of zero forward speed (due to the increase in viscosity when the forward speed decreases), and are observed more clearly for the smallest bilge keel height.

Tab. 6. Bilge keel (BK) heights and boundary layer thicknesses

Parameters	Ship (h_S)	h_S/δ	Model (h_M)	h_M/δ
Full BK height (h) [m]	0.45	1.5	0.0225	1.125
0.7 BK height [m]	0.315	1.05	0.01575	0.78
0.5 BK height [m]	0.225	0.75	0.01125	0.56
Boundary layer thickness (δ) [m]	0.3	-	0.02	-

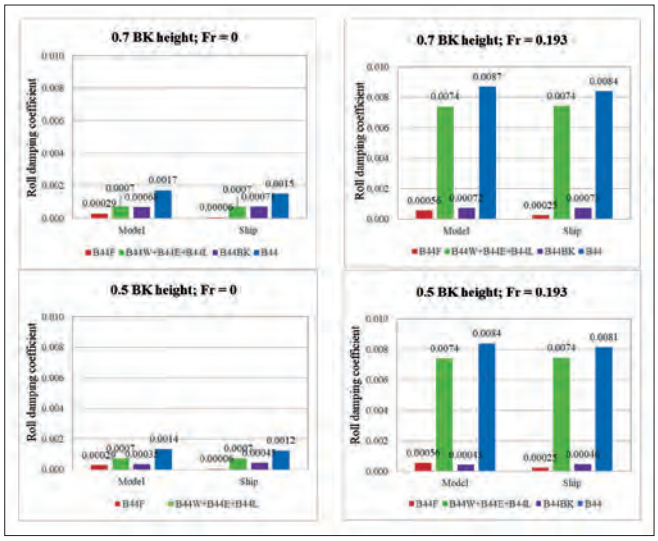

Fig. 7. Roll damping coefficients (comparison between ship and model)

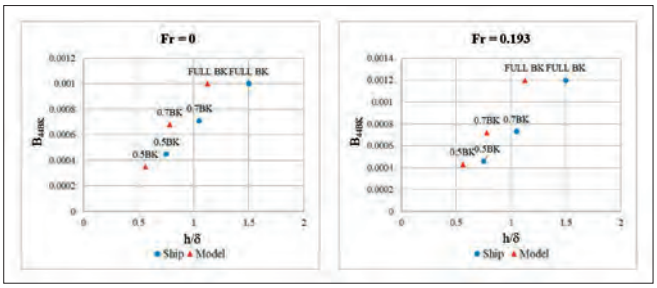

Fig. 8. Results for B_{44BK} and h/δ

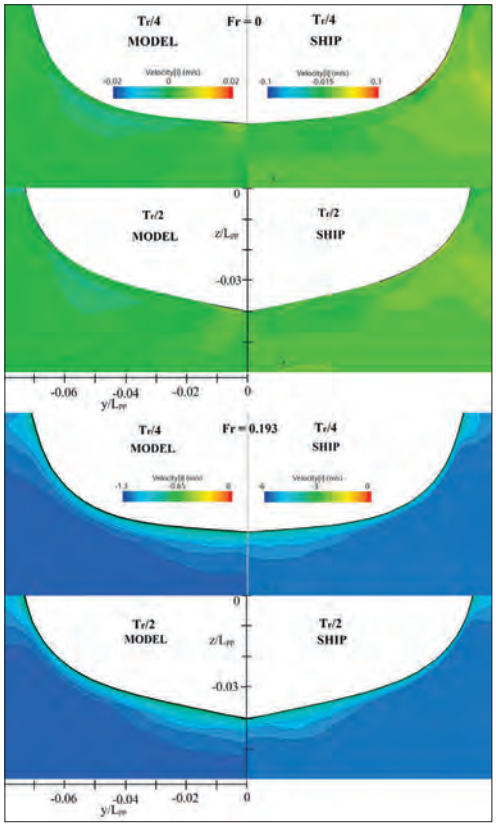

Fig. 9. Velocity fields (naked hull)

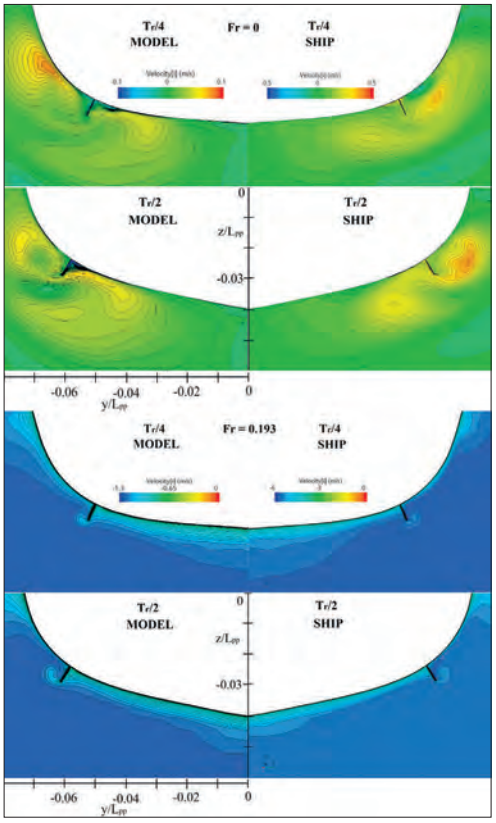

Fig. 10. Velocity fields (full BK height)

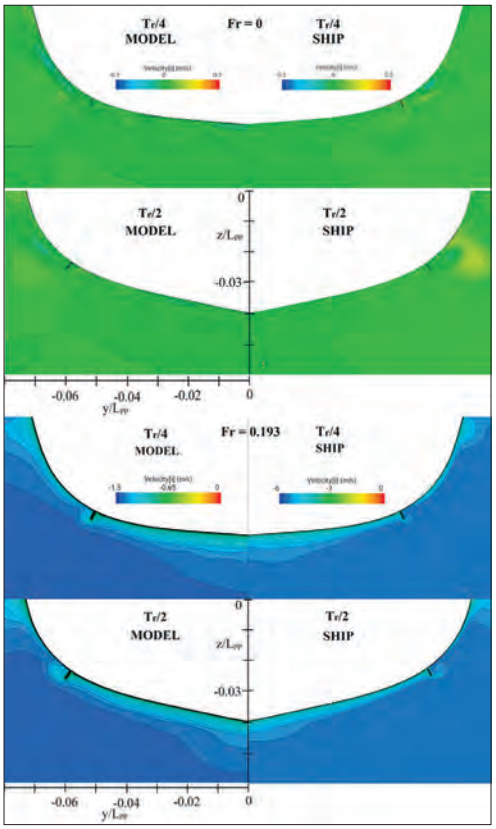

Fig. 11. Velocity fields (0.5 BK height)

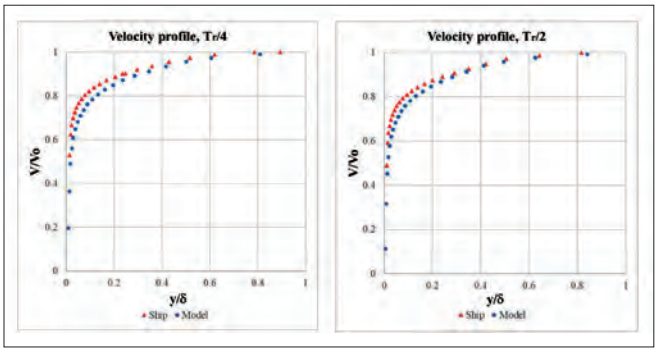

Fig. 12. Comparison of the velocity distributions in the boundary layer for the ship and model

In all cases, the boundary layer thickness at the model scale is larger than at the full scale (the thickness of the boundary layer increases with the viscosity of the fluid). In the case of a naked hull, the velocity fields at zero forward speed are different at the full scale and the model scale, due to the difference in the Reynolds number (viscosity). This is the reason for the scale effects on the frictional damping component. At the full bilge keel height, the velocity fields and vorticities are similar at the full scale and the model scale, meaning that the bilge keel damping component is not affected by scale effects. For half height, differences between the velocity fields at the model scale and the full scale can be seen. The vorticities at the full scale are observed more clearly than at the model scale; moreover, the velocity in the boundary layer of the ship is greater than that of the model (Figure12), whereas the bilge keel heights are the same (after geometric scaling). This explains why the bilge keel damping coefficient of the ship is larger than that of the model.

CONCLUSION

Using the Italian ship *Bettica*, full-scale and model-scale roll motions were simulated for different conditions and roll damping coefficients, and the velocity fields are obtained. The following conclusions can be drawn:

(1) The numerical results for the roll decay motions of both the model and ship are in good agreement with experimental data, meaning that our simulation strategy is reasonable. The numerical simulation strategy in this study can be used to predict roll motion for other vessels for which there are no experimental results.

(2) It is found that there are scale effects on roll decay motion that cause the difference in roll amplitudes between the model-scale and full-scale ships. The effects are larger at zero forward speed.

(3) Of the roll damping components, the frictional component in particular is affected by scale effects. The percentage of the frictional component is larger at the model scale and in the case of no forward speed. When the bilge keel height is reduced to a certain value that is smaller than the boundary layer thickness, the bilge keel component is also affected by scale effects. The bilge keel damping coefficient for the full-scale ship is larger than that of the model. In addition, the scale effects on the bilge keel component are larger in the case of no forward speed, and increase with a decrease in bilge keel height.

(4) The velocity fields around the bilge keels are similar in the full-scale and model-scale ships for full bilge keel height, while they are different in the case of half height. For half height, the vorticities at full scale are observed more clearly than at the model scale, which results in a greater velocity magnitude inside the boundary layer of the full-scale ship. Together with the larger boundary layer observed at the model scale, these are the reasons why the scale effects on bilge keel component occur when the bilge keel height is reduced.

In general, although the percentage of frictional component is not large in terms of the total roll damping, and is fairly small at the full scale, the viscous effect still causes a difference in roll amplitude between the model-scale and full-scale ships in the case of zero or low forward speed. If this is ignored, it may cause errors in roll motion predictions. However, these effects need to be studied further for other vessels with different scale ratios in the future.

ACKNOWLEDGEMENTS

This work was financially supported by JST SPRING, under grant number JPMJSP2139.

REFERENCES

1. Himeno Y. Prediction of ship roll damping–A state of the art. U. Michigan Dept. of Naval Arch. and Marine Engineering, Report 239, 1981.

2. Grant D J. Full Scale Investigation of bilge keel effectiveness at forward speed. M.Sc. dissertation. Faculty of Virginia Polytechnic Institute and State University, 2008.

3. Broglia R, et al. Experimental and numerical analysis of the roll decay motion for a patrol boat. Nineteenth International Offshore and Polar Engineering Conference, OnePetro, 2009. https://doi.org/10.5957/jsr.2009.53.4.179.

4. Kianejad S, et al. Investigation of scale effects on roll damping through numerical simulations. Proceedings of the 32nd Symposium on Naval Hydrodynamics, Hamburg, Germany, 2018.

5. Söder C-J, et al. Assessment of ship roll damping through full-scale and model-scale experiments and semi-empirical methods. 11th International Conference on the Stability of Ships and Ocean Vehicles, September 23–28, 2012. https://doi.org/10.1007/987-3-030-00516-0_10.

6. Retrieved February 24, 2007 from https://virtualglobetrotting.com/map/italian-commandante-class-light-combatant-ship-commandante-bettica-p492/.

7. Gu M, et al. Validation of CFD simulation for ship roll damping using one pure car carrier and one standard model. Proceedings of the 15th International Ship Stability Workshop, Stockholm, 2016.

8. Irkal M A, et al. Numerical prediction of roll damping of ships with and without bilge keel. Ocean Engineering 179, 226–245, 2019. https://doi.org/10.1016/j.oceaneng.2019.03.027.

9. Yong Z, et al. Turbulence model investigations on the boundary layer flow with adverse pressure gradients. Journal of Marine Science and Application 14(2), 170–174, 2015. https://doi.org/10.1007/s11804-015-1303-0.

10. ITTC Recommended Procedures and Guidelines. Practical guidelines for ship CFD applications, ITTC 7.5–03-02–03. Retrieved June, 2017 from https://www.ittc.info/media/9773/75-03-02-03.pdf.

11. Liu L, et al. CFD prediction of full-scale ship parametric roll in head wave. Ocean Engineering 233, 109–180, 2021. https://doi.org/10.1016/j.oceaneng.2021.109180.

12. Song K, et al. Simulation strategy of the full-scale ship resistance and propulsion performance. Engineering Applications of Computational Fluid Mechanics 15(1), 1321–1342, 2021. https://doi.org/10.1080/19942060.2021.1974091.

13. Song S, et al. An investigation into the effect of biofouling on the ship hydrodynamic characteristics using CFD. Ocean Engineering 175, 122–137, 2019. https://doi.org/10.1016/j.oceaneng.2019.01.056.

14. Terziev M, et al. Scale effects and full-scale ship hydrodynamics: A review. Ocean Engineering 245, 2022. https://doi.org/10.1016/j.oceaneng.2021.110496.

15. Tezdogan T, et al. Full-scale unsteady RANS simulations of vertical ship motions in shallow water. Ocean Engineering 123, 131–145, 2016. https://doi.org/10.1016/j.oceaneng.2016.06.047.

16. ITTC Recommended Procedures and Guidelines. Estimation of Roll Damping. ITTC 7.5-02-07-04.5. Retrieved June, 2021 from https://www.ittc.info/media/9759/75-02-07-045.pdf.

17. ITTC Recommended Procedures and Guidelines. Uncertainty Analysis in CFD Verification and Validation Methodology and Procedures. ITTC 7.5-03-01-01. Retrieved June, 2021 from https://www.ittc.info/media/9765/75-03-01-01.pdf .

18. Roache P J. Code verification by the method of manufactured solutions. J. Fluids Eng. 124(1), 4–10, 2002. https://doi.org/10.1115/1.1436090.

19. Zhou Y, et al. Direct calculation method of roll damping based on three-dimensional CFD approach. Journal of Hydrodynamics 27, 176–186, 2015. https://doi.org/10.1016/S1001-6058(15)60470-X.

20. Yıldız B, Katayama T. Bilge keel–free surface interaction and vortex shedding effect on roll damping. Journal of Marine Science and Technology 22, 432–446, 2017. https://doi.org/10.1007/s00773-016-0423-9.

21. Ikeda Y, et al. Components of roll damping of ship at forward speed. Journal of the Society of Naval Architects of Japan 143, 113–125, 1978.

22. Katayama T, et al. Characteristics of Roll Damping of Pure Car Carrier and Liquefied Natural Gas Carrier and Applicability of Ikeda's Method with some Modifications. Proceedings of the 1st International Conference on the Stability and Safety of Ships and Ocean Vehicles, Glasgow, Scotland, UK, 2021.

23. Cengel Y and Cimbala J. Fluid mechanics fundamentals and applications (si units). McGraw Hill; 2013.